

# Solutions of the Wheeler-Feynman equations with discontinuous velocities

Daniel Câmara de Souza<sup>1, a)</sup> and Jayme De Luca<sup>2, b)</sup>

<sup>1)</sup> *Universidade de São Paulo*

*Instituto de Física*

*Departamento de Física Matemática*

*Rua do Matão, Travessa R, N<sup>o</sup> 187*

*Caixa Postal 66.318, CEP 05508-090*

*São Paulo, São Paulo, Brasil*

<sup>2)</sup> *Universidade Federal de São Carlos,*

*Departamento de Física*

*Rodovia Washington Luis, km 235*

*Caixa Postal 676, CEP 13565-905*

*São Carlos, São Paulo, Brazil*

(Dated: 21 October 2021)

We generalize Wheeler-Feynman electrodynamics with a variational boundary-value problem with past and future boundary segments that can include velocity discontinuity points. Critical-point trajectories must satisfy the Euler-Lagrange equations of the action functional, which are neutral-differential delay equations of motion (the Wheeler-Feynman equations of motion). At velocity discontinuity points, critical-point orbits must satisfy the Weierstrass-Erdmann conditions of continuity of partial momenta and partial energies. We study a special class of boundary data having the shortest time-separation between boundary segments, for which case the Wheeler-Feynman equations reduce to a two-point boundary problem for an ordinary differential equation. For this simple case we prove that the extended variational problem has solutions with discontinuous velocities. We construct a numerical method to solve the Wheeler-Feynman equations together with the Weierstrass-Erdmann conditions and calculate some numerical orbits with discontinuous velocities.

PACS numbers: 02.30.Ks; 03.50.De; 05.45-a

## I. INTRODUCTION

To overcome the lack of equations of motion for point charges in Maxwell's electrodynamics, J. Wheeler and R. Feynman<sup>1,2</sup> developed an electrodynamics based on the minimization of the Fokker-Schwarzschild-Tetrode<sup>3-5</sup> action to replace Maxwell's equations. Besides having sensible equations of motion for point charges, the action functional seemed to point towards a canonical quantization<sup>6,7</sup> of the two-body problem, so far an unfulfilled promise<sup>8</sup>.

In a recent development, Wheeler-Feynman electrodynamics was embedded in a variational boundary-value problem<sup>9</sup>, henceforth variational electrodynamics<sup>10,11</sup>. The development of Ref.<sup>9</sup> was followed by a study of the neutral differential delay equations of motion of the electromagnetic two-body problem<sup>10,11</sup>.

Consistent application of variational electrodynamics defines trajectories with discontinuous velocities among the critical points of the variational problem<sup>10,11</sup>, henceforth broken extrema<sup>12</sup>. The conditions for a piecewise  $C^2$  extremal trajectory are (i) to satisfy the Euler-Lagrange equations along  $C^2$  segments, which are neutral differential delay equations, henceforth the Wheeler-Feynman equations of motion, and (ii) at velocity dis-

continuity points (henceforth breaking points), a broken extremum must further satisfy the Weierstrass-Erdmann continuity conditions for the partial momenta and partial energies<sup>11,12</sup>, a system of four nonlinear equations at each breaking point<sup>13</sup>. It is known that neutral differential delay equations can generate breaking points<sup>13</sup> which are propagated along trajectories<sup>14</sup>. As regards some physical property of the two-body problem, it can be shown that globally bounded two-body trajectories with vanishing far-fields *must* have discontinuous velocities<sup>10</sup>.

The electromagnetic variational problem<sup>9</sup> has boundary conditions in past and future, which make it hard to study numerically. Here we study the simplest boundary value problem, having the shortest possible time-distance between past and future boundary segments, as explained in the following. For these, the variational problem reduces to a two-point boundary problem<sup>11</sup> (i.e. a shooting problem for an ODE integrator<sup>15</sup>). We show well-posedness and calculate some numerical solutions of the variational problem with shortest-length segments near circular orbits of large radii<sup>16,17</sup>.

This paper is divided as follows: In Section II we introduce the variational boundary value problem. In Section III we explain the Weierstrass-Erdmann corner conditions for extrema with discontinuous velocities of the boundary-value problem with shortest-length boundary segments. In Section IV we develop the numerical method for shortest-type boundaries and calculate some numerical trajectories. In Section V we put the discussions and conclusion.

<sup>a)</sup> author's email address: [daniel.souza@usp.br](mailto:daniel.souza@usp.br)

<sup>b)</sup> author's email address: [jayme.deluca@gmail.com](mailto:jayme.deluca@gmail.com); webpage <https://sites.google.com/site/jaymedeluca/>

## II. VARIATIONAL BOUNDARY VALUE PROBLEM

Here we consider the natural electronic units where the speed of light, electronic charge and electronic mass are  $c = -e_1 = m_1 \equiv 1$ . We henceforth use the index  $i = 1$  to indicate electronic quantities and the index  $i = 2$  to denote quantities of the positive charge 2.

The variational problem is to find (extended) trajectories given by continuous and piecewise  $C^2$  functions of a (real) parameter  $s \rightarrow \mathbf{x}_i(s) \equiv (t_i(s), \mathbf{x}_i(s)) \in \mathbb{R} \times \mathbb{R}^3 \equiv \mathbb{R}^4$ . Henceforth a dot over vectors of  $\mathbb{R}^4$  denotes derivative respect to the parameter  $s$ , i.e.,  $\dot{\mathbf{x}}_i \equiv d\mathbf{x}_i/ds = (\dot{t}_i(s), \dot{\mathbf{x}}_i(s))$  for  $i = 1, 2$ . On regular segments the particle velocities are recovered by the chain rule,  $d\mathbf{x}_i/dt_i = \dot{\mathbf{x}}_i/\dot{t}_i$ . The space  $\mathbb{R}^4$  is equipped with the usual Euclidean norm of  $\mathbb{R}^4$  (double bars), defined by the inner product, i.e.,  $\|\mathbf{x}_i\|^2 \equiv \langle \dot{\mathbf{x}}_i | \dot{\mathbf{x}}_i \rangle \equiv \dot{t}_i^2 + |\mathbf{x}_i|^2$ , where single bars  $|\cdot|$  denote the Euclidean norm in  $\mathbb{R}^3$ . To each vector  $\mathbf{v} = (a, \mathbf{b}) \in \mathbb{R} \times \mathbb{R}^3$  we define its dual by  $\mathbf{v}^\dagger \equiv (a, -\mathbf{b})$ . A form that appears often is the (real) Minkowski bilinear form between two vectors  $\mathbf{v}_1 \equiv (a_1, \mathbf{b}_1)$  and  $\mathbf{v}_2 \equiv (a_2, \mathbf{b}_2)$ , defined by the scalar product with the other vector's dual, i.e.,  $\langle \mathbf{v}_1 | \mathbf{v}_2^\dagger \rangle \equiv a_1 a_2 - (\mathbf{v}_1 \cdot \mathbf{v}_2)$ , where dot denotes the scalar product of  $\mathbb{R}^3$ .

Central to the construction of the variational problem are the light-cone conditions

$$t_{j\pm}(s_j) = t_i(s) \pm |\mathbf{x}_i(s) - \mathbf{x}_j(s_j)|, \quad (1)$$

for  $j \equiv 3 - i$  and  $i = 1, 2$ , which are implicit conditions for the trajectories. In Eq. (1) the plus sign defines the future light-cone condition for particle  $i$ , while the minus sign defines the past light-cone condition for particle  $i$ . In Ref.<sup>19</sup> it is shown that if trajectories are *sub-luminal*, i.e.,

$$\left| \frac{d\mathbf{x}_i}{dt_i} \right| < 1, \quad (2)$$

for  $i = 1, 2$ , the light-cone conditions (1) have unique solutions  $s_{j\pm}(s)$ . Henceforth a  $\pm$  sign after the particle index  $j \equiv 3 - i$  indicates a quantity of particle  $j$  evaluated at the advanced/retarded argument  $s_{j\pm}(s)$ .

The variational two-body problem<sup>9</sup> is defined by the critical-point conditions of the action functional

$$S := \int_{s_{O^+}}^{s_{L_B}} K_2 ds_2 + \int_{s_{O_A}}^{s_{L^-}} K_1 ds_1 + \int_{s_{O_A}}^{s_{L^+}} U_{12}^- ds_1 + \int_{s_{O_A}}^{s_{L^-}} U_{12}^+ ds_1, \quad (3)$$

where

$$K_i := m_i \left( 1 - \sqrt{\langle \dot{\mathbf{x}}_i | \dot{\mathbf{x}}_i^\dagger \rangle} \right), \quad (4)$$

and the interaction energy

$$U_{ij}^\pm(\mathbf{x}_i, \mathbf{x}_{j\pm}, \dot{\mathbf{x}}_i, \dot{\mathbf{x}}_{j\pm}) := -\frac{e_i e_j \langle \dot{\mathbf{x}}_i | \dot{\mathbf{x}}_{j\pm}^\dagger \rangle}{2|\langle \mathbf{x}_i - \mathbf{x}_{j\pm} | \dot{\mathbf{x}}_{j\pm}^\dagger \rangle|}, \quad (5)$$

with  $i = 1, 2$  and  $j \equiv 3 - i$ , which has a non-zero denominator along non-collisional trajectories<sup>19</sup>. Henceforth we specify for the attractive problem by setting  $e_i e_j = -1$  in Eq. (5). The first variation of (3) naturally decomposes in a sum of two partial variations,  $\delta S = \delta S_1 + \delta S_2$ , as follows; (i) for variation  $\delta S_1$  trajectory 1 varies for  $s_1 \in [s_{O_A}, s_{L^-}]$  while trajectory 2 is kept fixed, and therefore the first term on the right-hand-side of (3) is a constant term,  $I_1$ . The remaining three integrals are over  $ds_1$ ,

$$S := I_1 + \int_{s_{O_A}}^{s_{L^-}} \mathcal{L}_1(\mathbf{x}_1, \mathbf{v}_1, \mathbf{x}_2, \mathbf{v}_2) ds_1, \quad (6)$$

thus defining the partial Lagrangian  $\mathcal{L}_1$  as the integrand, and (ii) along variation  $\delta S_2$  trajectory 2 varies for  $s_2 \in [s_{O^+}, s_{L_B}]$  while trajectory 1 is kept fixed. To calculate variation  $\delta S_2$  it is convenient to express functional (6) with three integrals over  $ds_2$ , plus a constant term  $I_2$ , as obtained using a change of variable on the last two integrals of Eq. (3) to the other particle's parameter in light-cone condition (1)<sup>11</sup>. Since the problem thus defined is totally symmetric, below we explain the critical point conditions and equations of motion for particle 1 only. Form (6) with its integral over partial Lagrangian  $\mathcal{L}_1$  is used to calculate the partial variation  $\delta S_1$  and the Euler-Lagrange equations of motion of particle 1.

The boundary conditions in past and future are described in Fig. 1, i.e. (a) the initial point  $O_A$  of trajectory 1 plus the boundary-segment of trajectory 2 from point  $O^-$  in the past-light-cone of  $O_A$  up to point  $O^+$  in the future light-cone of  $O_A$  (dashed black triangle on the left-hand-side of FIG. 1), and (b) the final point  $L_B$  of trajectory 2 plus the boundary-segment of trajectory 1 inside the endpoints  $(L^-, L^+)$  in the past/future light-cone condition of  $L_B$  (dashed black triangle on the right-hand-side of FIG. 1).

Since past and future boundary segments are supposed to be independent of each other, we must have that the past boundary-segment of particle 2 does not interact with the future boundary-segment of particle 1, in which minimal case point  $L^-$  is in the forward light-cone condition of point  $O^+$ .

Next we discuss the variational problem for piecewise  $C^2$  continuous trajectories  $\mathbf{x}_1(s)$ ,  $\mathbf{x}_2(s)$  having monotonically increasing time-components and satisfying the above boundaries conditions. To calculate the first variation  $\delta S_1$  we assume trajectory  $\mathbf{x}_i(s)$  and its continuous perturbation  $\mathbf{b}_1(s)$  are  $C^2$  inside the intervals  $s_i \in (s_{\mu-1}, s_\mu)$  defined by the grid of possible discontinuities  $s_\mu$  with  $\mu = 1, \dots, N$ . The perturbed trajectory is defined by

$$\mathbf{u}_i(s) = \mathbf{x}_1(s) + \mathbf{b}_1(s), \quad (7)$$

and outside the grid of discontinuity points,  $s \neq s_\mu$ ,

$$\dot{\mathbf{u}}_i(s) = \dot{\mathbf{x}}_1(s) + \dot{\mathbf{b}}_1(s), \quad (8)$$

and for  $i = 1$  satisfy the fixed-ends boundary conditions

$$\mathbf{b}_1(s_{O_A}) = \mathbf{b}_1(s_{L^-}) = 0. \quad (9)$$

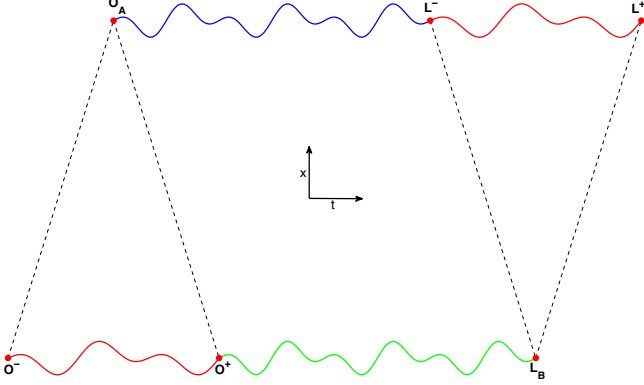


FIG. 1. The boundary conditions in  $\mathbb{R} \times \mathbb{R}^3$  are (a) initial point  $O_A \equiv (s_{O_A}, \mathbf{x}_1(s_{O_A}))$  of trajectory 1 and the respective elsewhere boundary segment of  $\mathbf{x}_2(s_2)$  for  $s_2 \in [s_{O^-}, s_{O^+}]$  (solid red line); (b) endpoint  $L_B \equiv (s_{L_B}, \mathbf{x}_2(s_{L_B}))$  of trajectory 2 and the respective elsewhere boundary segment of  $\mathbf{x}_1(s_1)$  for  $s_1 \in [s_{L^-}, s_{L^+}]$  (solid red line). Trajectories  $\mathbf{x}_1(s_1)$  for  $s_1 \in [s_{O_A}, s_{L^-}]$  (solid blue line) and  $\mathbf{x}_2(s_2)$  for  $s_2 \in [s_{O^+}, s_{L_B}]$  (solid green line) are determined by the extremum condition. Arbitrary units.

The first variation  $\delta S_i$  induced by a trajectory variation (7) about a non-collisional sub-luminal trajectory is<sup>19</sup>

$$\begin{aligned} \delta S_i &= \sum_{\mu=1}^{\mu=M} \int_{s_{\mu-1}}^{s_\mu} \left[ \left\langle \frac{\partial \mathcal{L}_i}{\partial \mathbf{x}_i} \middle| \mathbf{b}_i \right\rangle + \left\langle \frac{\partial \mathcal{L}_i}{\partial \mathbf{v}_i} \middle| \dot{\mathbf{b}}_i \right\rangle \right] ds_i \\ &\quad + \mathcal{O}(\|\mathbf{b}_i\|^2), \end{aligned} \quad (10)$$

where  $\|\mathbf{b}_i\|$  is the norm of piecewise  $C^2$  perturbations,

$$\|\mathbf{b}_i\| := \sup \|\mathbf{b}_i\| + \text{ess sup } \|\dot{\mathbf{b}}_i\| + \text{ess sup } \|\ddot{\mathbf{b}}_i\|, \quad (11)$$

Integrating (10) by parts over each  $C^2$  segment to eliminate the integral containing  $\dot{\mathbf{b}}_i(s)$  yields

$$\begin{aligned} \delta S_i &= \sum_{\mu=1}^{\mu=N} \int_{s_{\mu-1}}^{s_\mu} \left\langle \mathbf{b}_i(s) \left[ \frac{\partial \mathcal{L}_i}{\partial \mathbf{x}_i} - \frac{d}{ds} \left( \frac{\partial \mathcal{L}_i}{\partial \mathbf{v}_i} \right) \right] \right\rangle ds \\ &\quad + \sum_{\mu=1}^{\mu=N} \int_{s_{\mu-1}}^{s_\mu} \frac{d}{ds} \left\langle \mathbf{b}_i(s) \left| \frac{\partial \mathcal{L}_i}{\partial \mathbf{v}_i} \right. \right\rangle ds. \end{aligned} \quad (12)$$

Since the  $\mathbf{b}_i(s)$  are continuous and vanish at the end-points, the second term of Eq. (12) can be re-arranged as

$$\begin{aligned} \delta S_i &= \sum_{\mu=1}^{\mu=N} \int_{s_{\mu-1}}^{s_\mu} \left\langle \mathbf{b}_i(s) \left[ \frac{\partial \mathcal{L}_i}{\partial \mathbf{x}_i} - \frac{d}{ds} \left( \frac{\partial \mathcal{L}_i}{\partial \mathbf{v}_i} \right) \right] \right\rangle ds \\ &\quad - \sum_{\mu=1}^{\mu=N-1} \left\langle \mathbf{b}_i(s_\mu) \left| \Delta \left( \frac{\partial \mathcal{L}_i}{\partial \mathbf{v}_i} \right) \right. \right\rangle, \end{aligned} \quad (13)$$

where

$$\Delta \left( \frac{\partial \mathcal{L}_i}{\partial \mathbf{v}_i} \right) := \frac{\partial \mathcal{L}_i}{\partial \mathbf{v}_i} \Big|_{s_{\mu^+}} - \frac{\partial \mathcal{L}_i}{\partial \mathbf{v}_i} \Big|_{s_{\mu^-}}, \quad (14)$$

is the (possible) discontinuity of partial momentum  $i$ .

For a critical point we must have  $\delta S_i = 0$  for arbitrary  $\mathbf{b}_i(s)$ , and since the first term on the right-hand-side of (13) is an integral and the second term depends on the discrete values of  $\mathbf{b}_i(s_\mu)$  on the finite number of grid points, each must vanish independently, yielding (a) Euler-Lagrange equations piecewise, henceforth the Wheeler-Feynman equations of motion, which can be written for the spatial components as<sup>9</sup>

$$m_i \frac{d}{ds} \left( \frac{\mathbf{v}_i(s)}{\sqrt{1-\mathbf{v}_i^2(s)}} \right) = e_i [\mathbf{E}_j(s, \mathbf{x}_i(s)) + \mathbf{v}_i(s) \times \mathbf{B}_j(s, \mathbf{x}_i(s))]. \quad (15)$$

As shown in Eq. (29) of Ref.<sup>9</sup>, the fourth Euler-Lagrange equation (for the time component) vanishes identically if (15) holds. In Eq. (15), the  $\mathbf{E}_j$  and  $\mathbf{B}_j$  stand for the semi-sum of advanced and retarded Liénard-Wiechert fields of charge  $j$ <sup>18</sup>,

$$\mathbf{E}_j \equiv \frac{1}{2} (\mathbf{E}_j^- + \mathbf{E}_j^+), \quad \mathbf{B}_j \equiv \frac{1}{2} (\mathbf{B}_j^- + \mathbf{B}_j^+), \quad (16)$$

where the Liénard-Wiechert fields are defined by

$$\begin{cases} \mathbf{E}_j^\pm(s_i, \mathbf{x}_i) := \frac{\mathbf{u}_{ij\pm}(1-\mathbf{v}_{j\pm}^2)}{\kappa_{ij\pm} r_{ij\pm}^2} + \frac{\mathbf{n}_{ij} \times \{\mathbf{u}_{ij\pm} \times \dot{\mathbf{v}}_{j\pm}\}}{\kappa_{ij\pm} r_{ij\pm}}, \\ \mathbf{B}_j^\pm(s_i, \mathbf{x}_i) := \mp \mathbf{n}_{ij\pm} \times \mathbf{E}_j^\pm. \end{cases} \quad (17)$$

with

$$\kappa_{ij\pm} := 1 \pm \mathbf{v}_{j\pm} \cdot \mathbf{n}_{ij\pm}, \quad \mathbf{u}_{ij\pm} := \mathbf{n}_{ij\pm} \pm \mathbf{v}_{j\pm}. \quad (18)$$

Still in Eq. (17),  $\gamma_{j\pm} := (1-\mathbf{v}_{j\pm}^2)^{-1/2}$  while  $r_{ij\pm}$  is the distance in light-cone,  $r_{ij\pm} := |\mathbf{x}_i - \mathbf{x}_{j\pm}|$ , and the unit vector  $\mathbf{n}_{ij\pm} := (\mathbf{x}_i - \mathbf{x}_{j\pm})/r_{ij\pm}$  points from the advanced/retarded position  $\mathbf{x}_{j\pm}$  to the position  $\mathbf{x}_i$ . The vanishing of the second term on the right-hand-side of (13) imposes four continuity conditions at each grid point, henceforth the

Weierstrass-Erdmann corner conditions<sup>12</sup> of continuity of partial momenta and partial energies

$$\mathbf{P}_i := \frac{\partial \mathcal{L}_i}{\partial \mathbf{v}_i} \quad \text{and} \quad E_i := -\frac{\partial \mathcal{L}_i}{\partial t_i}. \quad (19)$$

Using definition (19) with Eq. (3) yields the partial momentum

$$\mathbf{P}_i := \frac{m_i \mathbf{v}_i}{\sqrt{\dot{t}_i - \mathbf{v}_i^2}} - \frac{\mathbf{v}_{j-}}{2r_{ij-}(\dot{t}_{j-} - \mathbf{n}_{ij-} \cdot \mathbf{v}_{j-})} - \frac{\mathbf{v}_{j+}}{2r_{ij+}(\dot{t}_{j+} + \mathbf{n}_{ij+} \cdot \mathbf{v}_{j+})}, \quad (20)$$

and the partial energy

$$E_i := \frac{m_i \dot{t}_i}{\sqrt{\dot{t}_i - \mathbf{v}_i^2}} - \frac{\dot{t}_{j-}}{2r_{ij-}(\dot{t}_{j-} - \mathbf{n}_{ij-} \cdot \mathbf{v}_{j-})} - \frac{\dot{t}_{j+}}{2r_{ij+}(\dot{t}_{j+} + \mathbf{n}_{ij+} \cdot \mathbf{v}_{j+})}. \quad (21)$$

Defining the right and left limits of the partial momenta/energies at each breaking point by  $\mathbf{P}_1^r, \mathbf{P}_1^l, E_2^r$  and  $E_2^l$ , respectively, the Weierstrass-Erdmann corner conditions can be expressed at each grid point  $s = s_\mu$  by

$$\begin{cases} \Delta \mathbf{P}_1 := \mathbf{P}_1^r - \mathbf{P}_1^l = \mathbf{0}, \\ \Delta \mathbf{P}_2 := \mathbf{P}_2^r - \mathbf{P}_2^l = \mathbf{0}, \\ \Delta E_1 := E_1^r - E_1^l = 0, \\ \Delta E_2 := E_2^r - E_2^l = 0. \end{cases} \quad (22)$$

### III. SHOOTING PROBLEM AND WEIERSTRASS-ERDMANN CORNER CONDITIONS

The shortest-length boundary value problem occurs when event  $L^-$  is in the future light-cone of event  $O^+$ , as illustrated in Fig. 2. Again, for boundaries with a smaller than the minimum time-separation illustrated in Fig. 2, the boundary-segments would interact in light-cone, an absurd.

For shortest-length boundary conditions, points  $\mathbf{x}_{2-}$  and  $\mathbf{x}_{1+}$  fall each on a past/future boundary segment (illustrated in red in Fig. 2), and therefore are given functions of the running positions  $\mathbf{x}_2$  and  $\mathbf{x}_1$ , thus reducing the Wheeler-Feynman equations to a two-point boundary problem for an ODE, as explained in the following.

The Wheeler-Feynman equations of motion (15) can be expressed as<sup>11</sup>

$$m_i \gamma_i \mathbf{a}_i = \frac{e_i}{2} [(\mathbf{v}_i \cdot \mathbf{E}_j^-)(\mathbf{n}_{ij-} - \mathbf{v}_i) + (1 - \mathbf{v}_i \cdot \mathbf{n}_{ij-})\mathbf{E}_j^- - (\mathbf{v}_i \cdot \mathbf{E}_j^+)(\mathbf{n}_{ij+} + \mathbf{v}_i) + (1 + \mathbf{v}_i \cdot \mathbf{n}_{ij+})\mathbf{E}_j^+], \quad (23)$$

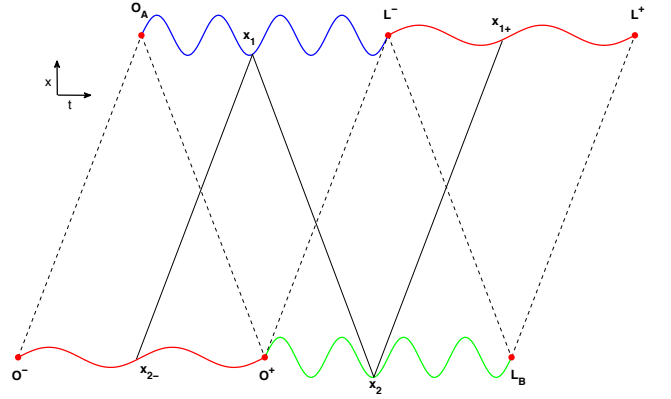


FIG. 2. Sketch of the space-time diagram for the boundary value problem with shortest-length boundaries. The variational problem is to find trajectories  $\mathbf{x}_1(t)$ , for  $t \in [t_{O^+}, t_{L^-}]$  (solid blue line), and  $\mathbf{x}_2(t)$ , for  $t \in [t_{O^-}, t_{L^+}]$  (solid green line), which match continuously with the boundary-segments  $\mathbf{x}_2(t)$  with  $t \in [t_{O^-}, t_{O^+}]$  and  $\mathbf{x}_1(t)$  with  $t \in [t_{L^-}, t_{L^+}]$ . The event  $O^+$  is in the past light-cone of  $L^-$ . Dashed and solid black lines connect points that are in the light-cone condition (either past or future).

where the fields  $\mathbf{E}_j^\pm$  can be re-arranged using (18) as

$$\mathbf{E}_j^\pm(t_i, \mathbf{x}_i) = \frac{\mathbf{u}_{ij\pm}}{\gamma_{j\pm}^2 \kappa_{ij\pm}^3 r_{ij\pm}^2} + \frac{(\mathbf{n}_{ij\pm} \cdot \mathbf{a}_{j\pm})\mathbf{u}_{ij\pm}}{\kappa_{ij\pm}^3 r_{ij\pm}} - \frac{\mathbf{a}_{j\pm}}{\kappa_{ij\pm}^2 r_{ij\pm}}. \quad (24)$$

The linear dependence of the  $\mathbf{E}_j^\pm$  on the accelerations  $\mathbf{a}_{j\pm}$  allows the use of a (simpler) matrix form

$$\mathbf{E}_j^\pm(t_i, \mathbf{x}_i) = \mathbf{D}_{ij\pm} \mathbf{u}_{ij\pm} + \mathbf{B}_{ij\pm} \mathbf{a}_{j\pm}, \quad (25)$$

where

$$\mathbf{D}_{ij\pm} := \frac{e_j \mathbb{1}}{\gamma_{j\pm}^2 \kappa_{ij\pm}^3 r_{ij\pm}^2}, \quad \text{and} \quad \mathbf{B}_{ij\pm} := \frac{e_j [\mathbf{u}_{ij\pm} \mathbf{n}_{ij\pm}^\top - \kappa_{ij\pm} \mathbb{1}]}{\kappa_{ij\pm}^3 r_{ij\pm}}. \quad (26)$$

Further using (18), Eq. (23) thus becomes

$$m_i \gamma_i \mathbf{a}_i = \mathbf{K}_{-ij} \mathbf{E}_j^- + \mathbf{K}_{+ij} \mathbf{E}_j^+, \quad (27)$$

where

$$\mathbf{K}_{\pm ij} := \frac{e_i}{2} [\mathbf{u}_{\pm ij} \mathbf{v}_i^\top + \kappa_{\pm ij} \mathbb{1}]. \quad (28)$$

We can isolate the accelerations  $\mathbf{a}_1$  and  $\mathbf{a}_2$  from Eqs. (23) with  $i = 1, 2$ , yielding an algebraic-differential equation

$$\begin{cases} (M_1 M_2 \mathbb{1} - \mathbf{A}_{12}^+ \mathbf{A}_{21}^-) \mathbf{a}_1 = \mathbf{A}_{12}^+ \mathbf{F}_1^+ + M_2 \mathbf{F}_2^-, \\ (M_1 M_2 \mathbb{1} - \mathbf{A}_{21}^- \mathbf{A}_{12}^+) \mathbf{a}_2 = \mathbf{A}_{21}^- \mathbf{F}_2^- + M_1 \mathbf{F}_1^+, \end{cases} \quad (29)$$

where we have defined the matrices

$$\begin{cases} \mathbf{F}_2^- := \mathbb{K}_{-12}(\mathbb{D}_{12-}\mathbf{u}_{12-} + \mathbb{B}_{12-}\mathbf{a}_{2-}) + \mathbb{K}_{+12}(\mathbb{D}_{12+}\mathbf{u}_{12+}), \\ \mathbf{F}_1^+ := \mathbb{K}_{+21}(\mathbb{D}_{21+}\mathbf{u}_{21+} + \mathbb{B}_{21+}\mathbf{a}_{1+}) + \mathbb{K}_{-21}(\mathbb{D}_{21-}\mathbf{u}_{21-}), \end{cases} \quad (30)$$

and  $M_i := m_i\gamma_i$ ,  $\mathbb{A}_{12}^+ := \mathbb{K}_{+12}\mathbb{B}_{12+}$  and  $\mathbb{A}_{21}^- := \mathbb{K}_{-21}\mathbb{B}_{21-}$ . If one can invert the matrices on the left-hand-side of (29) locally, the *algebraic differential equation* (29) reduces to an ODE.

In order to be able to invert the matrices on the left-hand-side of (29),

$$\begin{cases} \mathbf{G}_{12} := (M_1M_2\mathbf{1} - \mathbb{A}_{12}^+\mathbb{A}_{21}^-), \\ \mathbf{G}_{21} := (M_1M_2\mathbf{1} - \mathbb{A}_{21}^-\mathbb{A}_{12}^+), \end{cases} \quad (31)$$

we restrict to boundary-segments satisfying

$$M_1M_2 \gg \frac{1}{r_{12+}r_{12-}\kappa_{12+}^3\kappa_{12-}^3}. \quad (32)$$

For example, along small perturbations of segments of circular orbits with large radii,  $r_{ij\pm} \gg 1^{16}$ , condition (32) holds.

Notice that the running accelerations in (29) are each defined respect to a different independent time variable, i.e.,  $\mathbf{a}_1 \equiv d^2\mathbf{x}_1/dt_1^2$  and  $\mathbf{a}_2 \equiv d^2\mathbf{x}_2/dt_{2+}^2$ , where  $t_{2+}(t_1)$  is defined by the implicit-function theorem and the future light-cone relation (1). The derivative  $dt_{2+}/dt_1$  is obtained by taking a derivative of (1) piecewise, yielding

$$\lambda_{12+} := \frac{dt_{2+}}{dt_1} = \frac{(1 + \mathbf{n}_{12+} \cdot \mathbf{v}_1)}{(1 + \mathbf{n}_{12+} \cdot \mathbf{v}_{2+})}. \quad (33)$$

Last, if (32) holds we can define the vector fields

$$\begin{cases} \mathbf{H}_{12} := \mathbf{G}_{12}^{-1}(\mathbb{A}_{12}^+\mathbf{F}_1^+ + M_2\mathbf{F}_2^-), \\ \mathbf{H}_{21} := \mathbf{G}_{21}^{-1}(\mathbb{A}_{21}^-\mathbf{F}_2^- + M_1\mathbf{F}_1^+), \end{cases} \quad (34)$$

and transform (29) into the following non-autonomous ODE

$$\begin{cases} \dot{\mathbf{v}}_1 = \mathbf{H}_{12}(t_1, \mathbf{x}_1, \mathbf{v}_1, \mathbf{x}_2, \mathbf{v}_2), \\ \dot{\mathbf{v}}_2 = \lambda_{12+}(t_1)\mathbf{H}_{21}(t_1, \mathbf{x}_1, \mathbf{v}_1, \mathbf{x}_2, \mathbf{v}_2), \\ \dot{\mathbf{x}}_1 = \mathbf{v}_1, \\ \dot{\mathbf{x}}_2 = \lambda_{12+}(t_1)\mathbf{v}_2, \end{cases} \quad (35)$$

with the two-point boundary conditions

$$\begin{aligned} \mathbf{x}_1(t_{O_A}) &= \mathbf{x}_{O_A}, & \mathbf{x}_1(t_{L^-}) &= \mathbf{x}_{L^-}, \\ \mathbf{x}_2(t_{O^-}) &= \mathbf{x}_{O^-}, & \mathbf{x}_2(t_{L_B}) &= \mathbf{x}_{L_B}, \end{aligned} \quad (36)$$

thus defining a two-point boundary problem. The factor  $\lambda_{12+}$  in Eq. (35) insures the running positions satisfy the  $t_1$ -explicit condition (1), thus arriving at the end-point with  $\mathbf{x}_2(t_{L_B})$  in the future light-cone of  $\mathbf{x}_1(t_{L^-})$  (the second column of boundary condition (36)).

We solve the two-point boundary problem (35) and (36) with a shooting method that searches initial velocities  $\mathbf{v}_1(t_{O_A})$ ,  $\mathbf{v}_2(t_{O^-}^r)$  at initial positions  $\mathbf{x}_{O_A}$ ,  $\mathbf{x}_{O^-}$  such that the initial value problem terminates at the specified end-points  $\mathbf{x}_{L^-}$ ,  $\mathbf{x}_{L_B}$ .

To define the map for the shooting method, we consider that position  $\mathbf{X} \equiv [\mathbf{x}_1, \mathbf{x}_2]^T$  at time  $t_{L^-}$  depends on the initial velocity  $\mathbf{V} \equiv [\mathbf{v}_1, \mathbf{v}_2]^T$ , i.e.  $\mathbf{X} = \mathbf{X}(t_{L^-}, \mathbf{V})$ , and linearize about some reference initial velocity,  $\mathbf{V}_0 \equiv [\mathbf{v}_{10}, \mathbf{v}_{20}]^T$ , yielding

$$\mathbf{X} = \mathbf{X}_0 + \mathbb{J}_{s0}(\mathbf{V} - \mathbf{V}_0). \quad (37)$$

Restricted to small perturbations of circular boundary segments, the velocity is a constant at  $O(1/r_{12})$ . The shooting method is used with (37) to numerically calculate matrix  $\mathbb{J}_{s0}$  and vector  $\mathbf{X}_0$  for the perturbed boundary data. For that we solve *seven* initial value problems (35) for the shooting map (37). The seven initial velocities  $\mathbf{V}$  are used with the same small perturbation of boundary segments from a large radius circular orbit, defined as follows; (a) we start with the velocity of the unperturbed circular orbit, for which the second term on the right-hand-side of (37) vanishes, thus calculating the constant  $\mathbf{X}_0$  within the numerical precision, and (b) we perturb each of the six components of the initial velocity away from the circular orbit's velocity  $\mathbf{V}_0$ , one component at a time. We further solve Eq. (37) for  $\mathbf{V}$ , substitute  $\mathbf{V}_0$  by  $\mathbf{V}$  and solve again the seven initial value problems (35) to find the new  $\mathbf{X}_0$  and  $\mathbb{J}_{s0}$ . This iterative process results in the following map

$$\mathbf{V}_k = \mathbf{V}_{k-1} + \mathbb{J}_{sk}^{-1}(\mathbf{X}_k - \mathbf{X}_{k-1}), \quad (38)$$

with  $k = 1, 2, \dots$  and  $\mathbf{X}_k = [\mathbf{x}_{L^-}, \mathbf{x}_{L_B}]^T$ . If for each iteration  $k$  the matrix  $\mathbb{J}_{sk}$  is well conditioned and the map (38) converges, these velocities solve the two-point boundary problem given by (35) and (36) within the numerical error.

The condition number of the shooting matrix depends on the stability of the initial value problem<sup>15</sup> and with generic boundary segments one may not be able either to invert matrix  $\mathbb{J}_{sk}$  or to find a unique solution or any solution for map (38). As we show next, for small perturbations of circular orbits of large radii the boundary value problem is well-posed in a local subspace of boundary segments, matrix  $\mathbb{J}_{sk}$  is well conditioned and iteration (38) converges. In general, we expect the orbital velocities at points  $\mathbf{O}^+$  and  $\mathbf{L}^-$  to be different from the velocity on the boundary segments, and thus *discontinuous*.

In Theorem 1 we analyze the condition of matrix  $\mathbb{J}_{sk}$  and the convergence of map (38) for boundary-segments near segments of circular orbits of large radii.

**Theorem 1** Let  $\mathbf{x}_i^S(t) \in \mathbb{R}^3$  and  $\mathbf{v}_i^S(t) \in \mathbb{R}^3$ , denote the positions and velocities along a doubly circular orbit<sup>16</sup>, and  $\mathbf{x}_i^h(t) \in \mathbb{R}^3$  be the boundary-segments for  $i = 1, 2$ . Assume the  $\mathbf{x}_i^h(t)$  are  $C^2$  and in a neighborhood of circular orbits with large radii,  $r_{12} \gg 1$ . Then the two-point boundary problem posed by ODE (35) with boundary conditions (36) has a unique solution that can be found using the shooting method.

**Proof.** The positions are given by the integral

$$\mathbf{X}(t_{L^-}) = \mathbf{X}(t_{O_A}) + \int_{t_{O_A}}^{t_{L^-}} \mathbf{V}(t) dt, \quad (39)$$

and for boundary segments near circular orbits with large radii, the velocity  $\mathbf{V}(t)$  is almost constant because the acceleration falls at the most as  $1/r_{12}$ , as can be found by inspecting (23) and (24). Notice that for near-circular boundary data of the shortest type the time span of the circular flight is so short that the trajectories are almost straight lines.

Using the above we have the approximation

$$\mathbf{X}(t_{L^-}) \cong \mathbf{X}(t_{O_A}) + \mathbf{V} \Delta t. \quad (40)$$

where  $\Delta t = t_{L^-} - t_{O_A}$ ,  $\mathbf{X}(t_{O_A}) = [\mathbf{x}_1^S(t_{O_A}), \mathbf{x}_2^S(t_{O_A})]^\top$ ,  $\mathbf{X}(t_{L^-}) = [\mathbf{x}_1^S(t_{L^-}), \mathbf{x}_2^S(t_{L^-})]^\top$  and  $\mathbf{V}$  is a constant vector. Approximating  $\mathbf{V}$  by the initial circular velocity  $\mathbf{V}_0 = [\mathbf{v}_1^S(t_{O_A}), \mathbf{v}_2^S(t_{O_A})]^\top$  yields

$$\mathbf{X}_0 = \mathbf{X}(t_{O_A}) + \mathbf{V}_0 \Delta t \quad (41)$$

and Eqs. (40) and (41) yield

$$\mathbf{X} = \mathbf{X}_0 + \Delta t(\mathbf{V} - \mathbf{V}_0). \quad (42)$$

Comparing (42) with (37) yields (37) with  $\mathbf{J}_{s_0} = \Delta t \mathbf{1}$ , where  $\Delta t$  is the time span and  $\mathbf{1}$  the  $6 \times 6$  identity matrix. Therefore matrix  $\mathbf{J}_{s_0}$  has a well-conditioned inverse and the unique solution depends continuously on the boundary segments and initial velocities, i.e., a well-posed shooting method (38). ■

When the continuous boundary-segments are only piecewise  $C^2$  and have velocity discontinuities, one has to stop the integration of ODE (35) at all breaking points to satisfy the Weierstrass-Erdmann corner conditions (22), as follows.

For boundary segments with pre-specified jumps, the Weierstrass-Erdmann corner conditions (22) form an overdetermined system of 8 equations for the 6 velocities  $\mathbf{v}_1^r$ ,  $\mathbf{v}_2^r$  to continue the orbit on the right-hand-side of each discontinuity point. The former shows that for generic boundary segments the solution may not even exist.

In order to describe boundary segments that *do have* solutions with nontrivial discontinuous velocities, we include as variables two components of each right-velocity along each boundary segment,  $\mathbf{v}_{2-}^r$ ,  $\mathbf{v}_{1+}^r$ , which have not been used until the corner point. Next we show that such augment of the set of variables must be made very carefully.

The above described augment generates an underdetermined nonlinear system having 8 equations and 12 variables,

$$\begin{cases} \Delta \mathbf{P}_1(\mathbf{v}_1^r, \mathbf{v}_2^r, \mathbf{v}_{1+}^r, \mathbf{v}_{2-}^r) = \mathbf{0}, \\ \Delta \mathbf{P}_2(\mathbf{v}_1^r, \mathbf{v}_2^r, \mathbf{v}_{1+}^r, \mathbf{v}_{2-}^r) = \mathbf{0}, \\ \Delta E_1(\mathbf{v}_1^r, \mathbf{v}_2^r, \mathbf{v}_{1+}^r, \mathbf{v}_{2-}^r) = 0, \\ \Delta E_2(\mathbf{v}_1^r, \mathbf{v}_2^r, \mathbf{v}_{1+}^r, \mathbf{v}_{2-}^r) = 0, \end{cases} \quad (43)$$

where the superscripts  $l, r$  denote the left-limit and right-limit of the velocities at the breaking points. Defining the velocity jumps  $\Delta \mathbf{v}_i := \mathbf{v}_i^r - \mathbf{v}_i^l$ , the vector of jumps  $\bar{\mathbf{v}} := (\Delta \mathbf{v}_1, \Delta \mathbf{v}_2, \Delta \mathbf{v}_{1+}, \Delta \mathbf{v}_{2-})^\top$  and the local value of the continuous vector  $\mathbf{d} := (\mathbf{P}_1^l, \mathbf{P}_2^l, E_1^l, E_2^l)^\top$  we can rewrite Eq. (43) as

$$\mathbf{F}(\bar{\mathbf{v}}) = \mathbf{d}. \quad (44)$$

Equations (20) and (21) are analytic functions of the velocities, thus yielding a locally convergent Taylor series for  $\mathbf{F}(\bar{\mathbf{v}})$  in powers of the jump vector  $\bar{\mathbf{v}} := (\Delta \mathbf{v}_1, \Delta \mathbf{v}_2, \Delta \mathbf{v}_{1+}, \Delta \mathbf{v}_{2-})^\top$ . Expanding about some velocity  $\bar{\mathbf{v}}_0$  yields

$$\mathbf{F}(\bar{\mathbf{v}}_0) + \bar{\mathbf{J}}_0(\bar{\mathbf{v}}_0)(\bar{\mathbf{v}} - \bar{\mathbf{v}}_0) + \mathcal{O}(|\bar{\mathbf{v}} - \bar{\mathbf{v}}_0|^2) = \mathbf{d}. \quad (45)$$

Defining  $\bar{\mathbf{f}}_0 \equiv \mathbf{d} - \mathbf{F}(\bar{\mathbf{v}}_0)$ , we obtain at lowest order a linear system of 8 equations for 12 variables,

$$\bar{\mathbf{J}}_0(\bar{\mathbf{v}}_0)(\bar{\mathbf{v}} - \bar{\mathbf{v}}_0) = \bar{\mathbf{f}}_0. \quad (46)$$

Next we analyze the linear system (46) for near-circular boundary segments of large radii. The idea is to choose four of the twelve variables on the left-hand-side of (46) as independent variables to be placed on the right-hand side of (46). The system thus generated should have an invertible linear  $8 \times 8$  matrix with maximum row rank on the left-hand-side, yielding a unique solution for the eight ‘‘slave variables’’ on the left-hand-side, i.e.,

$$\mathbf{J}_0(\mathbf{v}_0)(\mathbf{v} - \mathbf{v}_0) = \mathbf{f}_0. \quad (47)$$

Vector  $\mathbf{f}_0 \equiv \mathbf{d} - \mathbf{F}(\mathbf{v}_0)$  on the right-hand-side of (47) should depend on the four independent variables, and for a non-trivial discontinuity,  $\mathbf{f}_0$  must be nonzero.

We solve (46) for  $\bar{\mathbf{v}}$  using the following iterative process. Starting from the solution  $\mathbf{v}$  of linear system (47),

we replace  $\mathbf{v}_0$  by  $\mathbf{v}$  and recalculate  $\mathbb{J}_0(\mathbf{v}_0)$  and  $\mathbf{f}$  to find the next iterate  $\mathbf{v}$  by (47), thus generating the following map

$$\mathbf{v}_{k+1} = \mathbf{v}_k + \mathbb{J}_k^{-1}(\mathbf{v}_k)\mathbf{f}_k, \quad (48)$$

with  $k = 0, 1, 2, \dots$  and  $\mathbf{f}_k \equiv \mathbf{d} - \mathbf{F}(\mathbf{v}_k)$ .

Theorem 2 gives an example where linear system (47) has a well conditioned matrix  $\mathbb{J}_0$  on the left-hand-side and a nonzero  $\mathbf{f}_0$ , thus determining a unique solution to (43) by iterating map (48).

**Theorem 2** Let  $(\mathbf{x}_i^S(t), \mathbf{v}_i^S(t)) \in \mathbb{R}^3$  denote positions and velocities along a doubly circular orbit<sup>16</sup>, and  $(\mathbf{x}_i^h(t), \mathbf{v}_i^h(t)) \in \mathbb{R}^3$  be the  $C^2$  boundary-segments in a neighbourhood of circular orbits with large radii,  $r_{12} \gg 1$ , for  $i = 1, 2$  and with  $\mathbf{v}_2^h(t)$  along the  $\hat{x}$  axis and  $\mathbf{v}_1^h(t)$  along the  $-\hat{x}$  axis. Then we can choose the  $x$  and  $z$  components of  $\Delta\mathbf{v}_1^h(t)$  and  $\Delta\mathbf{v}_2^h(t)$  as independent variables. The reduced linearized problem for the remaining (slave) variables  $\mathbf{v} \equiv (\Delta\mathbf{v}_1, \Delta\mathbf{v}_2, \Delta v_{1+}^y, \Delta v_{2-}^y)^\top$  is an inhomogeneous linear system given by (48) with a well-conditioned matrix  $\mathbb{J}_k$ , yielding a unique solution to Eq. (43).

**Proof.** For the above described near-circular orbits with a large inter-particle separation,  $r_{12\pm} \equiv r \gg 1$ , and low velocities,  $v_{1\pm}^r = v_{2\pm}^r \equiv v^r \ll 1$ , we have  $\mathbf{n}_{12+} \approx \mathbf{e}_y$ ,  $\mathbf{n}_{12-} \approx \mathbf{e}_y$ ,  $\mathbf{v}_{2-}^r = v^r \mathbf{e}_x$ ,  $\mathbf{n}_{21+} \approx \mathbf{n}_{21-} = -\mathbf{e}_y$ ,  $v_{1+}^r = -v^r \mathbf{e}_x$ . The linearized expansion (47) evaluated in the limit of large radii where trajectories are approximated by straight lines near  $\mathbf{v}_0 = \mathbf{0}$  yields  $\mathbf{f}_0 = -\frac{1}{2r}(\Delta v_{2-}^x, 0, \Delta v_{2-}^z, \Delta v_{1+}^x, 0, \Delta v_{1+}^z, 0, 0)^\top$  and

$$\mathbb{J}_0 = \begin{pmatrix} m_1 & 0 & 0 & -\frac{1}{2r} & 0 & 0 & 0 & 0 \\ 0 & m_1 & 0 & 0 & -\frac{1}{2r} & 0 & -\frac{1}{2r} & 0 \\ 0 & 0 & m_1 & 0 & 0 & -\frac{1}{2r} & 0 & 0 \\ -\frac{1}{2r} & 0 & 0 & m_2 & 0 & 0 & 0 & 0 \\ 0 & -\frac{1}{2r} & 0 & 0 & m_2 & 0 & 0 & -\frac{1}{2r} \\ 0 & 0 & -\frac{1}{2r} & 0 & 0 & m_2 & 0 & 0 \\ -m_1 v_1^r & 0 & 0 & 0 & \frac{1}{2r} & 0 & -\frac{1}{2r} & 0 \\ 0 & \frac{1}{2r} & 0 & m_2 v_2^r & 0 & 0 & 0 & -\frac{1}{2r} \end{pmatrix}. \quad (49)$$

Matrix  $\mathbb{J}_0$  is well-conditioned and one can calculate the next iterate  $\mathbf{v}_{k+1}$  using map (48) with  $k = 1$ . For a continuous dependence on boundary data, velocity discontinuities in histories can be chosen arbitrarily in the subspace of independent discontinuity variables,  $(\Delta v_{1+}^x, \Delta v_{2-}^x, \Delta v_{1+}^z, \Delta v_{2-}^z)$ . Thus restricted, matrix  $\mathbb{J}_k$  is invertible and the unique solution for the slave variables  $\mathbf{v} \equiv (\Delta\mathbf{v}_1, \Delta\mathbf{v}_2, \Delta v_{1+}^y, \Delta v_{2-}^y)^\top$  depends continuously on the boundary data and on  $(\Delta v_{1+}^x, \Delta v_{2-}^x, \Delta v_{1+}^z, \Delta v_{2-}^z)$  and the unique solution to (43) is given by the fixed point of map (48). ■

## IV. NUMERICAL EXPERIMENTS

The family of circular orbits<sup>16</sup> with angular velocity  $\omega$  and radius  $r_i = v_i/\omega$ , with  $i = 1, 2$ , can be parametrized by the retardation angle<sup>11</sup>  $\theta$ . The light-cone time  $\tau$  for light to travel the inter-particle distance is related to the constant retardation angle of the circular orbit by<sup>11</sup>  $\tau = \theta/\omega$ . In the limit of small  $\theta$ , the circular radii are given by  $r_i = 1/(m_i\theta^2)$  for  $i = 1, 2$  and the constant angular frequency is  $\omega = m_1 m_2 \theta^3 / (m_1 + m_2)$ <sup>11</sup>.

Our first numerical experiment uses boundary data given by a continuous perturbation of circular orbit's segments with  $\theta = 0.77$  for  $m_1 = 1$  and  $m_2 = 2$ , henceforth boundary data (I). The perturbed boundary segments include a velocity discontinuity in the middle of the histories, i.e., are only piecewise  $C^2$ . The numerical solution is calculated with a shooting method that solves each initial value problem (35) with a fourth-order Runge-Kutta method, as described in Section (III). When the integration reaches the breaking point the Runge-Kutta integrator is halted and we solve the Weierstrass-Erdmann corner conditions using the linear solution (47) as initial guess for the function `fsolve` of MatLab R2011a.

In Fig. 3 we show the trajectories of the particles, history segments in red and numerically calculated trajectories in black and blue lines. In Fig. 4 we show the components of the velocity of particle 1 and Fig. 5 shows the components of the velocity of particle 2. Notice that the numerically calculated solutions have discontinuous velocities at points  $\mathbf{O}^+$  and  $\mathbf{L}^-$  (which is a generic feature of the shortest-length boundaries) and at one extra pair of points in light-cone and along each trajectory as caused by the breaking point in histories.

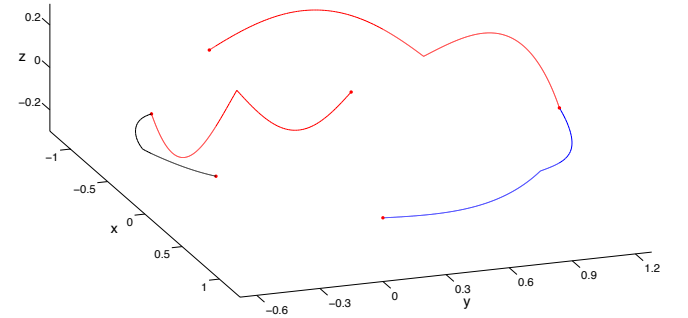


FIG. 3. Trajectories for boundary data (I) having a single velocity-discontinuity point and in a neighbourhood of a circular orbit with  $\theta = 0.77$ , for  $m_1 = 1$  and  $m_2 = 2$ . Trajectory of particle 1 (solid blue line) and the future history segment 1 (solid red line). Trajectory of particle 2 (solid black line) and the past history segment 2 (solid red line). Arbitrary units.

In our second numerical experiment the boundary segments are given by a  $C^2$  perturbation of circular orbit's segments with  $\theta = 0.077$  for  $m_1 = 1$  and  $m_2 = 10$ , henceforth boundary data (II). The perturbed boundary segments have no velocity discontinuity in the history segments. The numerical solution is again calculated with a shooting method that solves each initial value problem

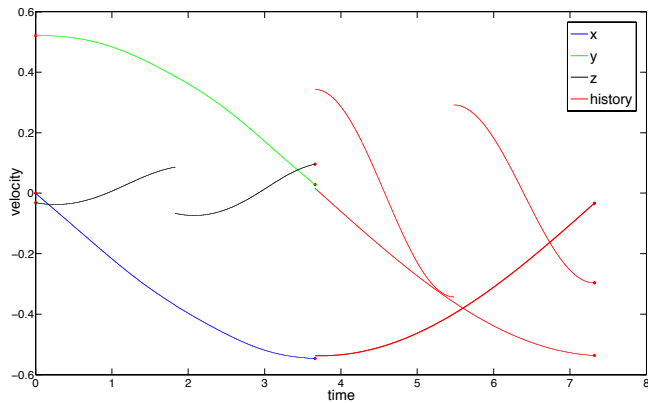


FIG. 4. Velocity of charge 1 for boundary data (I), having one breaking point and given by perturbation in a neighbourhood of the circular orbit with  $\theta = 0.77$ ,  $m_1 = 1$  and  $m_2 = 2$ . Arbitrary units.

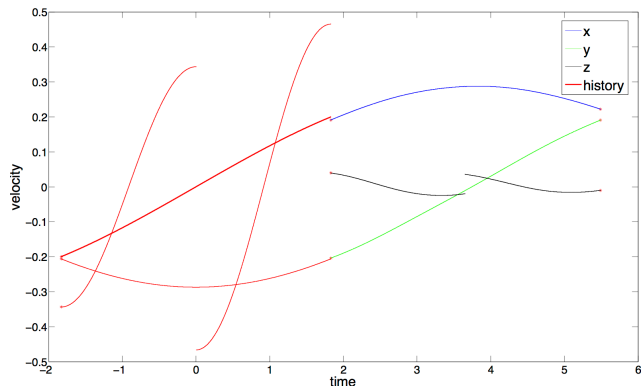


FIG. 5. Velocity of charge 2 for boundary data (I), having one breaking point and given by perturbation in a neighbourhood of a circular orbit with  $\theta = 0.77$ ,  $m_1 = 1$  and  $m_2 = 2$ . Arbitrary units.

(35) with a fourth-order Runge-Kutta method, as described in Section (III). In Fig. 6 we show the trajectories of the particles, history segments in red and numerically calculated trajectories in black and blue lines. Last, Fig. 7 shows the components of the velocity of particle 1 and Fig. 8 shows the components of the velocity of particle 2. Notice that for our second experiment the numerically calculated solutions have velocity discontinuities only at points  $O^+$  and  $L^-$ .

## V. DISCUSSIONS AND CONCLUSION

We studied the variational boundary value problem of the electromagnetic two-body problem with shortest-length boundary-segments in a neighbourhood of circular orbits with large inter-particle separations,  $r_{ij} \gg 1$ . The Wheeler-Feynman equations reduce to a two-point boundary problem, (35) and (36). For this case the initial value problem given by (35) is well-posed and the solution is unique (Theorem 1). We observed that the shooting method converged even for some perturbations

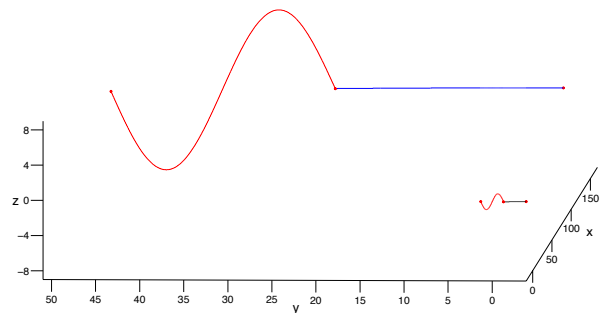


FIG. 6. Trajectories for boundary data (II) given by a  $C^2$  perturbation of a circular orbit with  $\theta = 0.077$ ,  $m_1 = 1$  and  $m_2 = 10$ . Trajectory of particle 1 (solid blue line) and the future history segment 1 (solid red line). Trajectory of particle 2 (solid black line) and the past history segment 2 (solid red line). Arbitrary units.

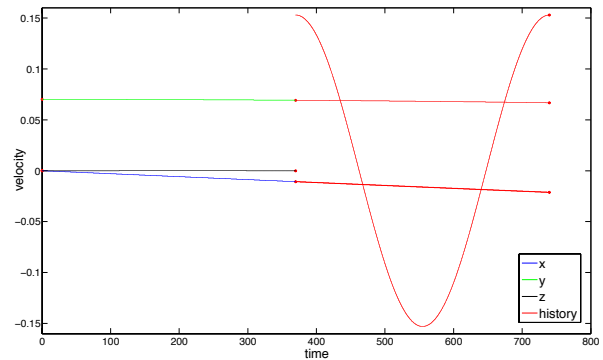


FIG. 7. Numerically calculated velocity of charge 1 for boundary data (II) given by a  $C^2$  perturbation of a circular orbit with  $\theta = 0.077$ ,  $m_1 = 1$  and  $m_2 = 10$ . Arbitrary units.

of circular orbits with radii  $r_{ij} \approx 0.5$  and having relativistic velocities  $v_i \approx 0.9$ , provided that  $|\mathbf{n}_{ij\pm} \cdot \mathbf{v}_{j\pm}| \approx 0.3$ .

The shooting problem uses up all the initial-velocity freedoms and the occurrence of discontinuous velocities at points  $O^+$  and  $L^-$  is expected even for  $C^2$  perturbations of circular-orbit segments (i.e., without breaking points in histories). We have also shown existence of solutions with discontinuous velocities for near-circular boundary-segments having discontinuous velocities in histories. For boundary-segments with continuous velocities, trajectories may still have discontinuous velocities satisfying Eq. (43) for inter-particle separation in the nuclear magnitude  $r_{12} \approx 1/\sqrt{m_1 m_2}$ , a case described by the algebraic-differential equation (29).

Situations where velocity discontinuities *necessarily* occur are (a) one of the boundary-segments has discon-



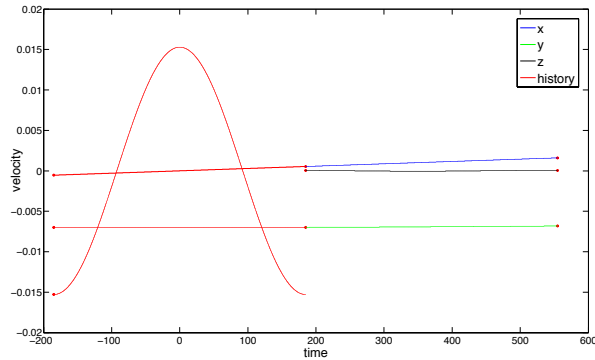


FIG. 8. Velocity of charge 2 for boundary data (II) given by a  $C^2$  perturbation of a circular orbit with  $\theta = 0.077$ ,  $m_1 = 1$  and  $m_2 = 10$ . Arbitrary units.

tinuous velocities, for example  $\Delta \mathbf{v}_{1+} = \mathbf{0}$  and  $\Delta \mathbf{v}_{2-} \neq \mathbf{0}$ . In this case Eq. (43) necessarily predicts  $\Delta \mathbf{v}_1 \neq \mathbf{0}$  and  $\Delta \mathbf{v}_2 \neq \mathbf{0}$  and (b) both boundary-segments have discontinuous velocities,  $\Delta \mathbf{v}_{1+} \neq \mathbf{0}$  and  $\Delta \mathbf{v}_{2-} \neq \mathbf{0}$ . For this case, Eq. (43) also predicts  $\Delta \mathbf{v}_1 \neq \mathbf{0}$  and/or  $\Delta \mathbf{v}_2 \neq \mathbf{0}$ .

## ACKNOWLEDGMENTS

Daniel Câmara de Souza acknowledges the support of FAPESP doctoral scholarship 2010/16964-0 and Jayme De Luca acknowledges the partial support of FAPESP regular grant 2011/18343-6.

<sup>1</sup>J. A. WHEELER AND R. P. FEYNMAN, Interaction with the Absorber as the Mechanism of Radiation. *Rev. Mod. Phys.* **17**, 157 (1945).

<sup>2</sup>J. A. WHEELER AND R. P. FEYNMAN, Classical Electrodynamics in Terms of Direct Interparticle Action. *Rev. Mod. Phys.* **21**, 425 (1949).

- <sup>3</sup>A. D. FOKKER, Ein invarianter Variationssatz für die Bewegung mehrerer elektrischer Massenteilchen. *Zeits. f. Physik* **58**, 386 (1929).
- <sup>4</sup>K. SCHWARZSCHILD, Zur Elektrodynamik. II. Die elementare elektrodynamische Kraft. *Göttinger Nachrichten* **128**, 132 (1903).
- <sup>5</sup>H. TETRODE, über den Wirkungszusammenhang der Welt. Eine Erweiterung der klassischen Dynamik. *Zeits. f. Physik* **10**, 317 (1922).
- <sup>6</sup>D. TER HAAR, The Old Quantum Theory. Pergamon Press, New York (1967).
- <sup>7</sup>C. M. ANDERSEN AND HANS C. VON BAEYER, Circular Orbits in Classical Two-Body Systems. *Annals of Physics* **60**, 67-84 (1970).
- <sup>8</sup>J. Mehra, J. MEHRA, The Beat of a Different Drum: Life and Science of Richard Feynman. Oxford University Press Inc., New York (1994).
- <sup>9</sup>J. DE LUCA, Variational Principle for the Wheeler-Feynman Electrodynamics. *J. Math. Phys.* **50**, 062701 (2009).
- <sup>10</sup>J. DE LUCA, Minimizers with discontinuous velocities for the electromagnetic variational method. *Phys. Rev. E* **82**, 026212 (2010).
- <sup>11</sup>J. DE LUCA, Variational electrodynamics of atoms. *Progress In Electromagnetics Research B.* **53**, 147-186 (2013).
- <sup>12</sup>I. M. GELFAND E S. V. FOMIN, Calculus of Variations. Prentice-Hall, Inc., Englewood Cliffs (1963).
- <sup>13</sup>A. BELLEN AND M. ZENNARO, Numerical Methods for Delay Differential Equations. Oxford University Press, New York (2003).
- <sup>14</sup>A. BELLEN AND N. GUGLIELMI, Solving neutral delay differential equations with state-dependent delays. *J. Comput. and App. Math.* **229**, 350-362 (2009).
- <sup>15</sup>U. M. ASCHER AND L. R. PETZOLD, Computer Methods for Ordinary Differential Equations and Differential-Algebraic Equations. SIAM, Philadelphia (1998).
- U. M. ASCHER, R. M. M. MATTHEIJ AND R. D. RUSSEL, Numerical Solution of Boundary Value Problems for Ordinary Differential Equations. SIAM, Englewood Cliffs (1995).
- <sup>16</sup>A. SCHILD, Electromagnetic Two-Body Problem. *Phys. Rev.* **131**, 2762 (1963).
- <sup>17</sup>M. SCHÖNBERG, Classical Theory of the Point Electron. *Phys. Rev.* **69**, 211 (1946).
- <sup>18</sup>J. D. JACKSON, Classical Electrodynamics. Third edition, John Wiley and Sons, New York (1999).
- <sup>19</sup>J. DE LUCA, T. HUMPRIES AND S. B. RODRIGUES, Finite Element Boundary Value Integration of Wheeler-Feynman Electrodynamics. *J. Comput. Appl. Math.* **236**(13), 3319-3337 (2012).